

# UC San Diego

## UC San Diego Previously Published Works

### Title

Fungal and herbivore elicitation of the novel maize sesquiterpenoid, zealexin A4, is attenuated by elevated CO<sub>2</sub>

### Permalink

<https://escholarship.org/uc/item/5nv5z7n3>

### Journal

Planta, 247(4)

### ISSN

0032-0935

### Authors

Christensen, Shawn A  
Huffaker, Alisa  
Sims, James  
[et al.](#)

### Publication Date

2018-04-01

### DOI

10.1007/s00425-017-2830-5

Peer reviewed



# Fungal and herbivore elicitation of the novel maize sesquiterpenoid, zealexin A4, is attenuated by elevated CO<sub>2</sub>

Shawn A. Christensen<sup>1</sup> · Alisa Huffaker<sup>2</sup> · James Sims<sup>3</sup> · Charles T. Hunter<sup>1</sup> · Anna Block<sup>1</sup> · Martha M. Vaughan<sup>4</sup> · Denis Willett<sup>1</sup> · Maritza Romero<sup>1</sup> · J. Erik Mylroie<sup>5</sup> · W. Paul Williams<sup>6</sup> · Eric A. Schmelz<sup>2</sup>

© Springer-Verlag GmbH Germany, part of Springer Nature 2017 (outside the usa) 2017

## Abstract

**Main conclusion** Chemical isolation and NMR-based structure elucidation revealed a novel keto-acidic sesquiterpenoid, termed zealexin A4 (ZA4). ZA4 is elicited by pathogens and herbivory, but attenuated by heightened levels of CO<sub>2</sub>.

The identification of the labdane-related diterpenoids, termed kauralexins and acidic sesquiterpenoids, termed zealexins, demonstrated the existence of at least ten novel stress-inducible maize metabolites with diverse antimicrobial activity. Despite these advances, the identity of co-occurring and predictably related analytes remains largely unexplored. In the current effort, we identify and characterize the first sesquiterpene keto acid derivative of  $\beta$ -macrocarpene, named zealexin A4 (ZA4). Evaluation of diverse maize inbreds revealed that ZA4 is commonly produced in maize scutella during the first 14 days of seedling development; however, ZA4 production in the scutella was markedly reduced in seedlings grown in sterile soil. Elevated ZA4 production was observed in response to inoculation with adventitious fungal pathogens, such as *Aspergillus flavus* and *Rhizopus microsporus*, and a positive relationship between ZA4 production and expression of the predicted zealexin biosynthetic genes, terpene synthases 6 and 11 (*Tps6* and *Tps11*), was observed. ZA4 exhibited significant antimicrobial activity against the mycotoxigenic pathogen *A. flavus*; however, ZA4 activity against *R. microsporus* was minimal, suggesting the potential of some fungi to detoxify ZA4. Significant induction of ZA4 production was also observed in response to infestation with the stem tunneling herbivore *Ostrinia nubilalis*. Examination of the interactive effects of elevated CO<sub>2</sub> (E-CO<sub>2</sub>) on both fungal and herbivore-elicited ZA4 production revealed significantly reduced levels of inducible ZA4 accumulation, consistent with a negative role for E-CO<sub>2</sub> on ZA4 production. Collectively, these results describe a novel  $\beta$ -macrocarpene-derived antifungal defense in maize and expand the established diversity of zealexins that are differentially regulated in response to biotic/abiotic stress.

**Keywords** Defense · Maize · Phytoalexin · Plant–microbe interactions · Zealexins

## Abbreviations

E-CO <sub>2</sub>	Elevated atmospheric carbon dioxide
HMBC	Heteronuclear multiple bond correlation
<i>Tps6/Tps11</i> (TPS6/TPS11)	Sesquiterpene synthases 6 and 11 genes (proteins)
ZA(ZB)	Zealexin A(B)

Shawn A. Christensen and Alisa Huffaker have been equally contributed to this article.

**Electronic supplementary material** The online version of this article (<https://doi.org/10.1007/s00425-017-2830-5>) contains supplementary material, which is available to authorized users.

✉ Shawn A. Christensen  
shawn.christensen@ars.usda.gov

✉ Eric A. Schmelz  
eschmelz@ucsd.edu

Extended author information available on the last page of the article

## Introduction

Biotic and abiotic stresses are significant limiting factors to maize production, resulting in billions of dollars in lost revenue annually in the US alone (Oerke et al. 1994; Savary et al. 2012; Mueller et al. 2016). Common elements of biotic stress include pathogenic and mycotoxigenic fungi such as members of the genus *Aspergillus* that infect maize ears and contaminate seed with potent carcinogens. Equally problematic are herbivores that consume leaf, root, and stem tissues including the European corn borer (*Ostrinia nubilalis*), which facilitates microbial colonization through the creation of contaminated feeding tunnels that promote stalk rot and disease (Keller et al. 1986; Gatch and Munkvold 2002). Abiotic stresses such as elevated atmospheric carbon dioxide (E-CO<sub>2</sub>) and other environmental stresses including heat and drought can further impact yield (Wang et al. 2003) and result in increased incidents of pathogenicity (Chakraborty and Newton 2011). For example, E-CO<sub>2</sub> is correlated with increases in *Fusarium pseudograminearum* crown rot in wheat (Melloy et al. 2010). Studies with maize grown at E-CO<sub>2</sub> demonstrated that kernel and stem tissues display increased susceptibility to the ear and stalk rot pathogen *Fusarium verticillioides* (Vaughan et al. 2014), an effect that was exacerbated by combining E-CO<sub>2</sub> with drought stress (Vaughan et al. 2016). Despite the documented impact of biotic and abiotic stress on maize production, relatively little is known about the numerous classes of specialized biochemical defenses in maize and the effect of abiotic stress on the production of these metabolites in planta.

Locally produced non-volatile terpenoids are inducible biochemical defenses that have been well-characterized in many dicot and monocot plant species (Ahuja et al. 2012; Schmelz et al. 2014). In maize, two classes of non-volatile terpenoids have been identified thus far, namely kauralexins (Schmelz et al. 2011) and zealexins (Huffaker et al. 2011). Kauralexins are kaurene-related derivatives of geranylgeranyl diphosphate produced by the *ent*-copalyl diphosphate synthase *Anther Ear 2* (*ZmAn2*), an ortholog of rice *ent*-copalyl diphosphate synthase genes that produce diterpenoid defenses (Watanabe et al. 1996; Harris et al. 2005). Characteristic of phytoalexins, kauralexins are pathogen- and insect-inducible and display strong antimicrobial activity (Schmelz et al. 2011).

Zealexins represent an additional biosynthetic class of non-volatile maize terpenoid defenses. Initial observations occurred in *Fusarium graminearum* infected stem tissues which revealed 14 novel analytes. Of the predictably related unknowns, four acidic sesquiterpenoids were elucidated via NMR and mass spectrometry, namely

zealexin A1, A2, A3 and B1 (Huffaker et al. 2011). Early insights into the biosynthesis of maize zealexins came from biochemical analyses demonstrating that the nearly identical sesquiterpene synthases 6 and 11 (TPS6/TPS11) cyclize farnesyl diphosphate to yield (*S*)- $\beta$ -bisabolene and ultimately (*S*)- $\beta$ -macrocarpene as a logical precursor to ZA1–3 and ZB1 (Basse 2005; Kollner et al. 2008). Correlations between *Rhizopus microsporus*-, *Aspergillus flavus*-, and *F. graminearum*-inducible *Tps6/Tps11* transcript abundance and zealexin production further supported a role for TPS6/TPS11 in zealexin biosynthesis (Huffaker et al. 2011). Additional advances in zealexin biosynthesis revealed that a cytochrome P450 mono-oxygenase (CYP71Z18) is capable of performing the enzymatic conversion of (*S*)- $\beta$ -macrocarpene to ZA1 (Mao et al. 2016); however, the *in vivo* role of CYP71Z18 remains to be demonstrated. Characterization of maize zealexins revealed that they are broadly pathogen inducible with ZA3 displaying the greatest abundance on average (Huffaker et al. 2011). Fungal growth bioassays with *R. microsporus*, *A. flavus*, and *F. graminearum* in liquid culture demonstrated that ZA1 and ZA3 have significant antimicrobial activity at physiologically relevant levels, consistent with a direct defensive role against fungal pathogens.

While strongly inducible biochemical defenses have been shown to play important roles following pathogen attack, only a limited number of studies have investigated the impact of abiotic stress on these responses in maize. Vaughan et al. (2014) demonstrated that *F. verticillioides*-infected stems and kernels have reduced defense levels in plants grown at E-CO<sub>2</sub> (800 ppm) compared to those grown under ambient conditions ([CO<sub>2</sub>] 400 ppm). Interestingly, analyses with E-CO<sub>2</sub> combined with drought stress enhanced maize phytoalexin defense responses to *F. verticillioides* (Vaughan et al. 2016). Other studies have shown that E-CO<sub>2</sub> can elicit both resistance (Kobayashi et al. 2006) and susceptibility (Strengbom and Reich 2006) responses, depending on the specific plant–microbe interaction. The variation in plant defense responses to different microbes under E-CO<sub>2</sub> highlights the need to investigate the rather unpredictable responses to other pathogens under abiotic stress conditions.

In our continuing investigation of maize defense responses to diverse fungal pathogens, we detected significant levels of an unknown analyte that chromatographed in the vicinity of known zealexins. Through chemical isolation and NMR-based structure elucidation, we identified a novel keto acid sesquiterpenoid, termed zealexin A4 (ZA4). Temporal and spatial regulation of ZA4 production in response to biotic stress was compared with *Tps6/Tps11* gene expression and the antimicrobial properties of ZA4 were investigated. Finally, we examined the impact of E-CO<sub>2</sub> on ZA4 production in response to individual challenge with pathogens and herbivores.

## Materials and methods

### Plant, insect and fungal material

Inbred maize lines (H88, Ms71, B73, CML247, I114H, Mo18W, CML277, CML322, CML52, CML288, TZi8, CML103, Oh43, CML69, Ki3, Hp301, M37W, Ki11, Ky21, Tx303, B97, NC350, CML333, W22, NC358) obtained from the National Genetic Resources Program, Germplasm Resources Information Network and hybrid maize (var. Golden Queen; Southern States Cooperative, Inc., Richmond, VA, USA) were grown in MetroMix® 200 (Sun Gro Horticulture Distribution Inc, Vancouver, BC, Canada) and supplemented with 14-14-14 Osmocote (Scotts Miracle-Gro, Marysville, OH, USA) as described in Schmelz et al. (2009). *Ostrinia nubilalis* (Benzon Research Inc., Carlisle, PA, USA) were reared on artificial diet at 29 °C and received as eggs or late first instars. Fungal stock cultures of *R. microsporus* (NRRL 54029) and *A. flavus* (NRRL 3357) were grown and spore inoculums were prepared as described by Huffaker et al. (2011).

### Zealexin A4 isolation and NMR analysis

*Zea mays* var. Golden Queen stems (6 kg) were cut in half lengthwise and subsequently inoculated and allowed to incubate for 5 days at room temperature in partially sealed plastic containers. Following incubation, samples were frozen in liquid nitrogen, ground to a coarse powder with a Champion Hammermill then ground to a fine powder in liquid nitrogen. This powder was then allowed to warm slightly and then was further ground in ethyl acetate. The resulting suspension was filtered through a Buchner funnel set up with a sorbent pad overlaid on filter paper. The resulting mixture was concentrated en vacuo on a Buchi rotovap (Buchi Corp., Newcastle, DE, USA). The extract was condensed directly onto C18 resin (20 g) and residual solvent removed en vacuo. The resulting impregnated C18 resin was used as a dry-loaded solid phase on a 5-g C18 flash column (RediSepRF Gold) using a Teledyne CombiFlash Rf (CombiFlash®Rf, Teledyne ISCO, Inc, Lincoln, NE, USA) in water: acetonitrile gradient with a flow rate of 18 mL min<sup>-1</sup>, with initiation at 20% acetonitrile for 5 min and proceeded to 100% acetonitrile over the next 60 min. This resulted in mixtures enriched in distinct phytoalexin classes. Chemical composition of fractions was monitored by GC/MS ESI analysis following TMS-diazomethane derivatization of the fractions. The fractions containing ZA4 were purified by prep HPLC on a Dionex Ultimate 3000 instrument equipped with a YMC-Pack OD-AQ column (250 × 20 mm, s-10 µm, 12 nm; Thermofisher,

Auburn, AL, USA). Each sample (20 mg) was eluted with water: acetonitrile gradient at a flow rate of 25 mL min<sup>-1</sup>. Careful fractionation of signals (UV 210) led to pure ZA4. The structure of ZA4 was elucidated using <sup>1</sup>H and <sup>13</sup>C APT 1D NMR experiments, as well as correlated spectroscopy (COSY), heteronuclear single quantum coherence (HSQC), and heteronuclear multiple bond correlation (HMBC) 2D experiments. Additional 2D experiments were performed to help resolve overlaying signals such as nuclear overhauser spectroscopy (NOESY), total correlation spectroscopy (TOCSY), HSQC-TOCSY and heteronuclear 2 bond correlation (H2BC). Data were collected on a Bruker Avance II 600 MHz cryoprobe (Bruker, Bellerica, MA, USA) as well as an Agilent 600 MHz <sup>13</sup>C direct detect cryoprobe (Agilent, Santa Clara, CA, USA). Data were analyzed using Mnova (MestreLab, Escondido, CA, USA) software. Assignment of chemical shifts were made directly from <sup>1</sup>H and <sup>13</sup>C APT data when possible, or inferred through 2D experiments, such as HSQC or HMBC.

### ZA4 quantification

ZA4 samples were solvent extracted, methylated, collected on a polymeric adsorbent using vapor-phase extraction (VPE), and analyzed using GC/isobutene chemical ion mass spectrometry (CI-MS) as previously described (Christensen et al. 2015). Metabolite quantification was based on U-<sup>13</sup>C-18:3 (Cambridge Isotope Laboratories, Inc, Tewksbury, MA, USA) as an internal standard.

### Antifungal activity assays

A modified version of the fungal growth assays described in the Clinical and Laboratory Standards Institute M38-A2 guidelines was used, as described by Schmelz et al. (2011). In brief, bioassays were carried out in liquid culture using an *A. flavus* or *R. microsporus* spore suspension (5 × 10<sup>4</sup> spores mL<sup>-1</sup>) in nutrient media containing 10, 50, or 100 µg mL<sup>-1</sup> ZA4 dissolved in DMSO (*n* = 8). Plates were incubated at 28 °C and fungal growth monitored by measuring an increase in absorbance (405 nm) in a BioTek Synergy4 instrument (BioTek Instruments Inc., Winooski, VT, USA) for 72 h.

### ZA4 elicitation assays

ECB treatments and fungal slit stems were carried out on 21–28-day-old greenhouse grown *Zea mays* var Golden Queen as previously described (Huffaker et al. 2011). For E-CO<sub>2</sub> ECB treatments, stems were infested with 3rd instar larvae by creating a hole in the second internode with a cork borer (#1) and caging the larvae in the infestation site with

copper mesh surrounding the hole. Four days post-infestation, stem sections surrounding the initial site of cork borer damage were harvested and tissue surrounding feeding tunnels was collected for analysis. E-CO<sub>2</sub> ECB stem treatments were carried out in a sunlit greenhouse using temperatures at 28 °C from 0700 h to 1900 h Eastern Standard Time (EST) followed by 1 h of smooth transition to 22 °C overnight as described in Vaughan et al. (2014). Air relative humidity was controlled between 55 and 60%. One greenhouse room was set at ambient 400 μmol CO<sub>2</sub> mol<sup>-1</sup> air, and the E-CO<sub>2</sub> room was kept at 800 μmol CO<sub>2</sub> mol<sup>-1</sup> air, which is the predicted global CO<sub>2</sub> concentration to be reached between 2080 and 2100 (Solomon et al. 2007). For scutella treatments, hybrid seed and inbred lines were germinated as described above and grown in sterile or non-sterile soil. Maize scutella were harvested at 2, 4, 6, 8, 10, and 12 days post-germination for time course experiments or at 10 days post-germination for diverse inbred lines or sterile/non-sterile soil experiments. For E-CO<sub>2</sub> kernel inoculations with *A. flavus* (strain NRRL 3357), methods were followed as described by Christensen et al. (2012), with the use of Conviron E15 (Conviron, Pembina, ND, USA) growth chambers controlled at 28 °C day/25 °C night with a 500 μmol m<sup>-2</sup> s<sup>-1</sup> photosynthetic photo flux density 12 h photoperiod and between 50 and 60% relative humidity, as described in Vaughan et al. (2014). One chamber was controlled at current at ambient 400 μmol CO<sub>2</sub> mol<sup>-1</sup> air, and the E-CO<sub>2</sub> room was kept at 800 μmol CO<sub>2</sub> mol<sup>-1</sup> air. Treatment groups were harvested in liquid N<sub>2</sub> 5 days post-inoculation for ZA4 analysis. For field analysis of *A. flavus*-infected kernels, the maize inbred line VA35 was planted in a five-row plot with 20 plants per row. The developing ears were inoculated with *A. flavus* strain NRRL 3357 or with sterile distilled water at 18 days after pollination using a size 12 quilting needle inserted into a pencil eraser. The husks were peeled back to expose the kernels prior to dipping the needle into a suspension of *A. flavus* (9 × 10<sup>7</sup> conidia mL<sup>-1</sup>) and inserting into the kernel through the seed coat at a depth of 2 mm. Following inoculation, the husks were re-positioned over the kernels, covered with a shoot bag, and secured with a rubber band. Kernels were harvested from at least three ears of each of the treatments at 3, 7, 14, and 21 days after inoculation. The kernels were flash frozen in liquid nitrogen and stored at - 80 °C.

## Statistical analysis

Analysis of variance (ANOVA) was carried out on quantified zealexin, ergosterol, and fungal growth levels. Log transformations were utilized when necessary after investigating adherence to assumptions of normality and homoscedasticity using visual inspections of quantile–quantile plots, residual diagnostics, Shapiro–Wilk’s test (normality) and Levene’s test (homoscedasticity). Post-hoc comparisons

of between-treatment differences were done using a Tukey’s HSD test. The relationships between pathogen-induced ZA4 production and fold change in gene expression for *Tps6* and *Tps11* were evaluated by applying a linear models fit on a log scale (i.e. log transformation of both ZA4 and fold change levels). Models were evaluated for goodness of fit, adherence to assumptions of normality and heteroscedasticity, *R*<sup>2</sup> values, and significance.

## Results

### Identity of a novel maize zealexin

While investigating maize terpenoid defenses present in *A. flavus*-infected stems and kernels, we observed an unclassified analyte in proximity to known zealexins (Fig. 1a). To identify this metabolite, chemical isolation was performed and the derivatized methylester of this native acidic

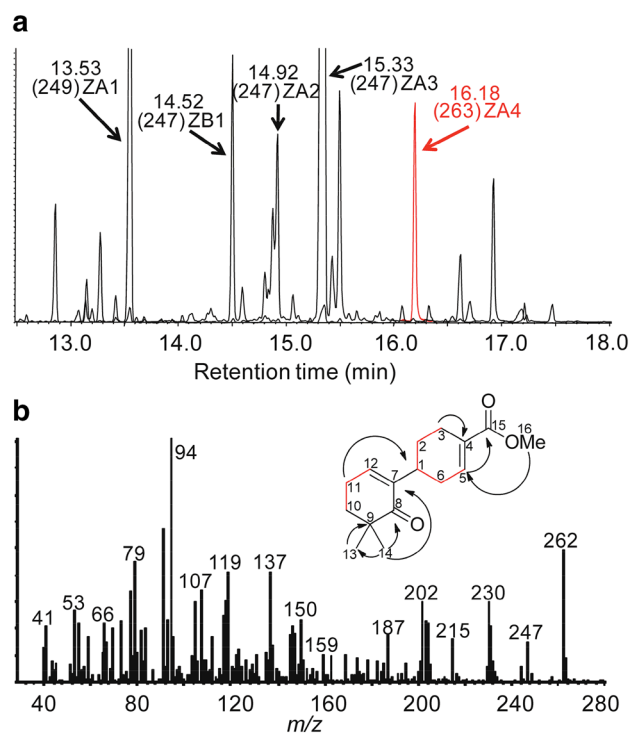


**Fig. 1** Identity and spectra of zealexin A4. **a** GC/CI-MS selected ion trace of fungal-induced acidic sesquiterpenoids as methyl ester derivatives. Labeled analytes include zealexin A1 (ZA1) [M+H]<sup>+</sup> 249 (white), zealexin B1 (ZB1) [M+H]<sup>+</sup> 247 (white); zealexins A2 and A3 (ZA2, ZA3) [M+H]<sup>+</sup> 247 (white); and zealexin A4 (ZA4) [M+H]<sup>+</sup> 263 (red). All unlabeled analytes are unknowns. **b** <sup>1</sup>H and <sup>13</sup>C NMR deduced zealexin A4 methyl ester structure and its electron ionization spectra (mass-to-charge ratio) shown as a methyl ester, y-axis denotes relative abundance of ions. In the ZA4 structure, COSY correlations are shown in red bonds and black arrows represent HMBC correlations



**Table 1** Annotated chemical shifts for each carbon atom of the zealexin A4 methylester

Position	$\delta^{13}\text{C}$ (ppm)	$\delta^1\text{H}$ (ppm)	HMBC	TOCSY
1	40.2	1H 1.67 (m)	C6, C7	–
2	25.7	2H 1.38 (m), 1.00 (m)	C1, C3, C4, C6, C7	C3, C5, C6
3	24.4	2H 2.47 (br d J = 17.7), 2.10 (br t 12.4)	C1, C2, C4, C5,	C2, C5, C6
4	130.7	–	–	–
5	137.6	1H 6.89 (m)	C3, C6, C11, C15	C2, C3, C6
6	29.5	2H 1.73 (m), 1.57 (m)	C1, C2, C4, C5,	C2, C3, C5
7	163.5	–	–	–
8	197.4	–	–	–
9	33.3	–	–	–
10	51.2	2H 2.05 (s)	C8, C9, C11, C12, C13, C14	C11, C12
11	41.5	2H 1.52 (s)	C1, C7, C8, C9, C10, C12, C13, C14	C10, C12
12	123.9	1H 5.83 (s)	C10, C11	C10, C11
13	27.7	3H 0.70 (s)	C7, C8, C9, C10, C11, C14	–
14	27.7	3H 0.70 (s)	C7, C8, C9, C10, C11, C13	–
15	167.3	–	–	–
16	50.8	3H 3.47 (s)	C4, C5	–

sesquiterpenoid was analyzed by  $^1\text{H}$  and  $^{13}\text{C}$  NMR (Fig. 1b; Table 1). The 1D  $^1\text{H}$  spectrum displayed three methyl groups with the gem-dimethyl group having overlapping signals at 0.70 ppm. The signals in the 2D phase-corrected heteronuclear single quantum coherence (HSQC) analysis were similar to those of other zealexins, revealing five quaternary carbons. The quaternary carbons were confirmed through correlations using a HMBC experiment. A clear  $^{13}\text{C}$  signal at 197.4 ppm denotes an  $\alpha,\beta$ -unsaturated ketone. Using correlated spectroscopy (COSY) analysis, partial ring systems were established, indicating the positions of the quaternary carbons. The placement of the ketone at carbon 8 is consistent with the corresponding alcohol group in zealexin A3 (Fig. 2) (Huffaker et al. 2011). The HMBC correlation from the methylester of the derivatized acid revealed the chemical shift of the acidic carbon as 167.3 ppm. Collectively, these results provide the basis for a novel sesquiterpenoid zealexin. Given the structural similarity to other zealexin A series metabolites, we termed the novel  $\beta$ -macrocarpene derivative zealexin A4 (ZA4). Positive electron ionization (EI) mass spectra of the corresponding ZA4 methyl ester derivative provide useful diagnostic fragments with a detectable  $m/z$  262  $[\text{M}]^+$  molecular ion (Fig. 1b). In a proposed model for zealexin biosynthesis (Fig. 2), initial steps begin with the cyclization of farnesyl diphosphate by TPS6/TPS11 into (*S*)- $\beta$ -bisabolene and ultimately  $\beta$ -macrocarpene. Formation of zealexin A1 results from a conversion of the C15 methyl group to a carboxylic acid potentially via a cytochrome P450 mono-oxygenase (CYP71Z18) (Mao et al. 2016). Conversions of ZA2 and ZA3 from ZA1 result from hydroxylation events at the C1 and C8 positions, respectively. Synthesis of ZA4 likely occurs via additional hydroxylation activity on ZA3, with the transformation of the C8 alcohol into a

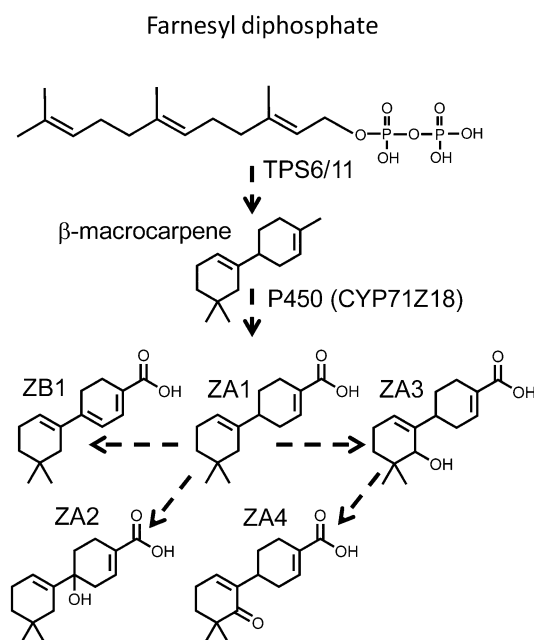


**Fig. 2** Proposed model of the zealexin biosynthesis pathway. Dashed arrows represent the predicted enzyme activities. Abbreviations are as follows: terpene synthases 6 and 11 (TPS6/TPS11), zealexins A1–A4, B1 (ZA1, ZA2, ZA3, ZA4, ZB1)

germinal diol that spontaneously dehydrates into a ketone (Greer et al. 2007).

### ZA4 accumulates in the scutella of developing seedlings

To investigate the temporal and spatial regulation of ZA4 production in untreated seedlings, we germinated seeds and

measured ZA4 concentrations in roots, shoots, and scutella tissues from hybrid maize (*Zea mays* var. Golden Queen) over a 14 d time course. ZA4 was virtually absent in root and shoot tissues over the 2-wk developmental period. However, appreciable levels ( $1.4 \mu\text{g g}^{-1}$  FW) were detected in scutella tissues 10 days post-germination (Fig. 3a). To determine the extent of natural variation in ZA4 production across maize varieties, we measured its production in scutella from 23 diverse parental inbreds used to develop the nested association mapping population (Yu et al. 2008). At 10 days post-germination, variable levels of ZA4 were observed with the highest concentrations detected in lines NC358 and NC350 ( $11.8$  and  $11.0 \mu\text{g g}^{-1}$  FW, respectively) and the lowest levels

in MS71 and II14H ( $0.6$  and  $1.3 \mu\text{g g}^{-1}$  FW, respectively; Fig. 3b). Comparison of all zealexins in scutella tissue between the 23 diverse inbred lines demonstrated varied levels of production (online resource S1), with diverse accumulation patterns between ZA3 and ZA4, suggesting that the conversion of ZA4 from ZA3 (Fig. 2) may not be spontaneous but enzymatic. To determine if ZA4 is developmentally regulated in maize scutella, we germinated seedlings under sterile and non-sterile soil conditions and measured ZA4 production 10 days post-germination. The accumulation of ZA4 was significantly higher in seeds grown in non-sterile soil (Fig. 3b), suggesting that ZA4 production is not regulated by developmental processes alone, but in response to biotic stimuli.

### Pathogen-inducible ZA4 has a positive relationship with *Tps6/Tps11* transcript accumulation and exhibits antimicrobial activity

To examine the pathogen inducibility of ZA4, we inoculated maize stems with *A. flavus* or *R. microsporus* and measured ZA4 production at 0, 4, 12, and 24 h post-inoculation (hpi). At 24 hpi, we observed significantly induced levels of ZA4 in both *A. flavus* and *R. microsporus*-infected tissues, with levels reaching  $2.0$  and  $1.6 \mu\text{g g}^{-1}$  FW, respectively, ( $P < 0.05$ ; Fig. 4a). Production of ZA4 was also elicited in a different plant–pathogen system, as *A. flavus*-infected kernels in the field produced  $> 30 \mu\text{g g}^{-1}$  FW at 14, and 21 days post-inoculation, surpassing levels of other zealexins at those time points by at least 2 to 6-fold (online resource S2). To examine the relationship between ZA4 production and the putative zealexin biosynthesis genes *Tps6* and *Tps11* (Huffaker et al. 2011), regression analyses were performed to compare levels of ZA4 in response to control, damage, *A. flavus*, and *R. microsporus* treatments with levels of *Tps6* and *Tps11* transcript accumulation. Figure 4b demonstrates a significant positive relationship between *A. flavus* and *R. microsporus*-elicited ZA4 production and *Tps11* (Adj.  $R^2 = 0.7464$ ,  $P < 0.0001$ ) and *Tps6* (Adj.  $R^2 = 0.5731$ ,  $P < 0.0001$ ) transcript accumulation. These results are consistent with the positive relationships exhibited by other zealexins and *Tps6/Tps11* expression (Huffaker et al. 2011) and the proposed role for TPS6 and TPS11 in zealexin biosynthesis.

Given the demonstrated antimicrobial properties of ZA1 and ZA3 (Huffaker et al. 2011), we hypothesized that ZA4 would have similar activities. To assess the antimicrobial activity of ZA4, we measured the growth of *A. flavus* in nutrient media containing different concentrations of ZA4 that fall within a physiologically relevant range (Fig. 4c; online resource S2). At  $10 \mu\text{g mL}^{-1}$ , ZA4 significantly inhibited the growth of *A. flavus* ( $P < 0.05$ ). Cultures with 50 and  $100 \mu\text{g mL}^{-1}$  concentrations of ZA4 displayed an even greater reduction in *A. flavus* growth,

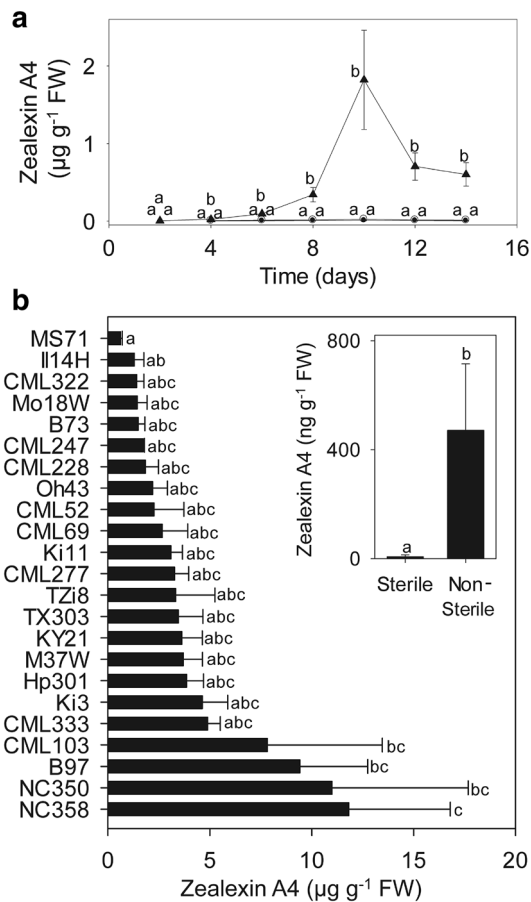


**Fig. 3** Zealexin A4 accumulates in the scutella of developing seedlings. **a** Average ( $n = 4$ ,  $\pm$  SE) ZA4 accumulation in the roots (open circle), shoots (closed circle), and scutella (closed triangle) of healthy untreated seedlings over a 14-day time course. **b** Average ( $n = 4$ ,  $\pm$  SE) ZA4 production detected in scutella of 10-day-old untreated seedlings from 23 parental inbred lines used to develop the nested association mapping population. Insert, average ( $n = 5$ ,  $\pm$  SEM) ZA4 accumulation in scutella from 10-day-old seedlings grown in sterile and non-sterile soil. Within plots, different letters (a–c) represent significant differences ( $P < 0.05$  for all ANOVAs;  $P < 0.05$  for Tukey test corrections for multiple comparisons)

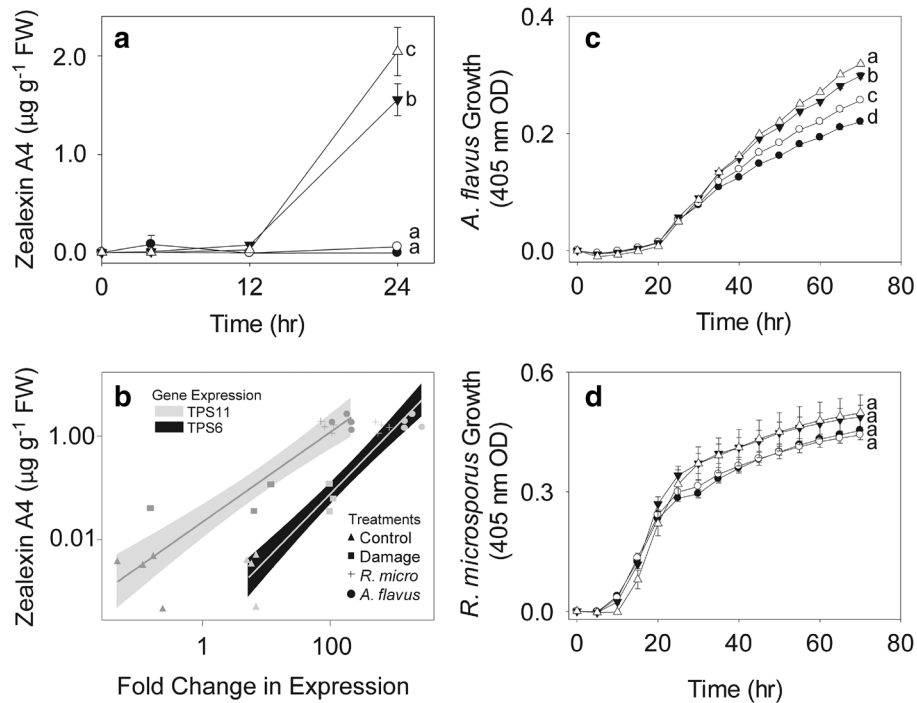


**Fig. 4** Pathogen-inducible zealexin A4 (ZA4) has a positive relationship with *Tps6* and *Tps11* transcript accumulation and displays antimicrobial activity against *A. flavus*. **a** Average ( $n = 4$ ;  $\pm$  SE) levels of ZA4 in stems in response to no treatment (open circle), damage plus water (closed circle), or damage plus water suspensions of *R. microsporus* (closed triangle), or *A. flavus* (open triangle), at 0 or 4, 12 and 24 h post-inoculation. **b** Observed relationship between pathogen-induced *Tps11* and *Tps6* transcript accumulation and ZA4 production in response to control (closed triangle), damage (closed square), *R. microsporus* (+), and *A. flavus* (closed circle) at 24 hpi. Grey and

black shaded areas represent 95% confidence intervals for *Tps11* and *Tps6* expression, respectively. **c, d** Fungal growth assays measuring antimicrobial activity of ZA4 against *A. flavus* (**c**) and *R. microsporus* (**d**). Average ( $n = 8$ ,  $\pm$  SE) fungal growth ( $OD_{405nm}$ ) in liquid culture containing nutrient broth with ZA4 at concentrations of 0 (open triangle), 10 (closed triangle), 50 (open circle), and 100 (closed circle)  $\mu\text{g mL}^{-1}$ . Within plots, different letters (a–d) represent significant differences ( $P < 0.05$  for all ANOVAs;  $P < 0.05$  for Tukey test corrections for multiple comparisons)

demonstrating a negative dose-dependent inhibition of fungal proliferation ( $P < 0.05$ ). In contrast to the antimicrobial effects of ZA4 on *A. flavus*, there was no significant inhibition of *R. microsporus* at any tested concentration of ZA4 in liquid cultures (Fig. 4d).

### ZA4 is elicited by the stem tunneling herbivore *O. nubilalis*

To determine if ZA4 is also elicited by herbivory, we infested maize stems with *O. nubilalis* and measured ZA4 production over a 12-day time course (Fig. 5). Four days post-infestation, ZA4 production was induced to levels significantly greater than the untreated controls ( $P < 0.05$ ). Following 8 days of *O. nubilalis* feeding, concentrations of ZA4 were significantly higher than both damage and untreated controls, and remained higher through the 12-day time course ( $P < 0.05$ ).

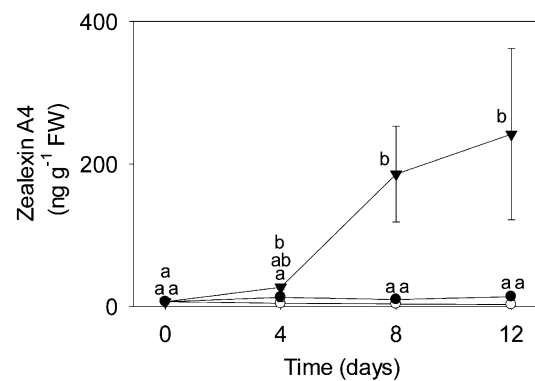


**Fig. 5** Elicitation of zealexin A4 (ZA4) by herbivory. Average ( $n = 3$ ,  $\pm$  SE) ZA4 accumulation in maize stems following no treatment control (open circle), damage (closed circle) or damage + *O. nubilalis* (closed triangle) over a 12-day time course. Within the plot, different letters (a–b) represent significant differences ( $P < 0.05$  for all ANOVAs;  $P < 0.05$  for Tukey test corrections for multiple comparisons)



## E-CO<sub>2</sub> has a strong negative impact on ZA4 production

As high levels of CO<sub>2</sub> can affect a plant's ability to respond to biotic threats (Vaughan et al. 2014), we examined the impact of E-CO<sub>2</sub> on ZA4 production during pathogen attack and herbivory. To determine if *A. flavus*-elicited ZA4 is impacted by E-CO<sub>2</sub>, mature maize kernels were infected with *A. flavus* both at ambient conditions (1× CO<sub>2</sub> = 400 ppm), and at concentrations twice that of normal atmospheric CO<sub>2</sub> (2× CO<sub>2</sub> = 800 ppm). Five days post-inoculation, a fivefold reduction in ZA4 was observed in *A. flavus*-infected kernels at 2× CO<sub>2</sub> compared to those at 1× CO<sub>2</sub>, suggesting a negative impact of E-CO<sub>2</sub> on ZA4 production (Fig. 6a), despite there being no difference in fungal growth (online resource S3). E-CO<sub>2</sub> also hampered ZA4 production in response to herbivory, with levels of ZA4 being fivefold lower in *O. nubilalis*-infested plants at 2× CO<sub>2</sub> compared to those grown at 1× CO<sub>2</sub> (Fig. 6b). Quantification of zealexins A1, B1, A2, and A3 in fungal- and herbivore-elicited plants revealed similar patterns for reduced metabolite levels in plants grown

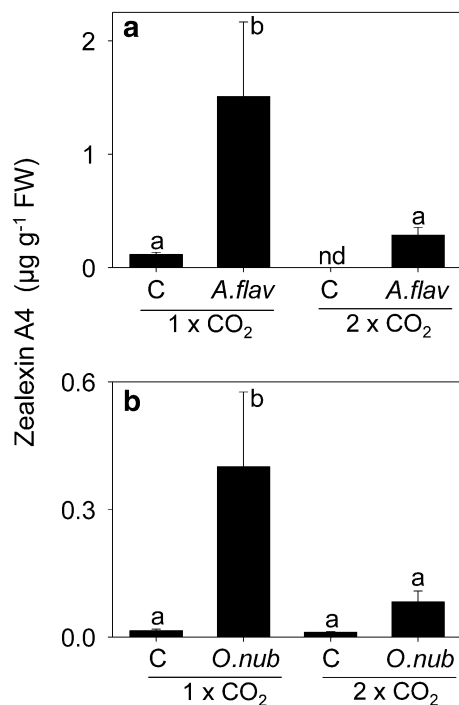


**Fig. 6** Impact of elevated CO<sub>2</sub> on fungal- and herbivore-induced zealexin A4. Average ( $n = 4$ ;  $\pm$  SE) levels of zealexin A4 in response to controls C, *A. flavus* (a), or *O. nubilalis* (b). Treatments were conducted under ambient (1× CO<sub>2</sub> = 400 ppm) or elevated CO<sub>2</sub> (2× CO<sub>2</sub> = 800 ppm) conditions. Within plots, different letters (a–b) represent significant differences, nd = no detection (all ANOVAs,  $P < 0.05$ ; Tukey test corrections for multiple comparisons,  $P < 0.05$ )

at E-CO<sub>2</sub> (online resource S4), suggesting a broad effect of E-CO<sub>2</sub> on biotic stress-induced zealexin production.

## Discussion

The profiling of phytoalexins in fungal-infected tissues led to the identification of a novel acidic sesquiterpenoid zealexin. <sup>1</sup>H and <sup>13</sup>C NMR analysis revealed a carboxylic acid-containing β-macrocarpene hydrocarbon skeleton that lacks a conjugated 1,1'3' triene system, and was thus classified as a constituent of the zealexin A series (Huffaker et al. 2011). Distinguished from other zealexin A compounds by its α,β-unsaturated ketone at the C-8 position, we termed the novel sesquiterpene keto acid as zealexin A4. The biosynthesis of ZA4 likely initiates with TPS6/TPS11 activity on farnesyl diphosphate to form ZA1 (Fig. 2). Evidence for the initial terpene synthase step in the ZA4 biosynthetic pathway was the positive relationship between *A. flavus*- and *R. microsporus*-elicited ZA4 production and *Tps6/Tps11* transcript accumulation. These results were similar to previous observations between total zealexin accumulation (ZA1, ZA2, ZA3, and ZB1) and *Tps6/Tps11* expression (Huffaker et al. 2011). The role of *Tps6/Tps11* in maize-microbe interactions was recognized previously, as expression (Doehlemann et al. 2008; Huffaker et al. 2011) and genetic studies (Basse 2005; Kollner et al. 2008; van der Linde et al. 2011) have convincingly characterized both genes to have functions in plant defense. The collective results from these studies coupled with our analyses suggest that TPS6/TPS11 are firm candidates for the redundant terpene synthases that cyclize the bicyclic sesquiterpenoid zealexin precursor, β-macrocarpene (Fig. 2) (Huffaker et al. 2011). The additional steps of ZA4 biosynthesis involves the conversion of ZA1 to ZA3 from hydroxylation activity on C8, followed by additional hydroxylation activity on ZA3 and further dehydrogenation to form a ketone at the C8 position. Our comparison of zealexin levels in the scutella of diverse inbred lines showed different ratios between ZA3 and ZA4 concentrations (online resource S1), indicating that the conversion of ZA3 to ZA4 may result from an enzymatic process rather than a spontaneous reaction.

ZA4 is ubiquitous in maize, as evidenced by quantifiable levels in the scutella of each diverse inbred line tested (Fig. 3b). As the scutella serves as the interface between the nutrient-rich endosperm and growing seedling, the presence of ZA4 and other maize terpenoids in this tissue (Huffaker et al. 2011; Schmelz et al. 2011) suggests the possibility that ZA4 is developmentally regulated, perhaps to thwart impending soil–microbe attack. This possibility was supported by the high expression levels of genes coding for enzymes that metabolize lipids and sequester reactive oxygen species (e.g. lipases, peroxidases, and catalases) in

scutella during the first 10 days of seedling development (Chandlee and Scandalios 1984; Wang and Huang 1987; Corona-Carrillo et al. 2014). Our analysis of seedlings germinated in sterile or non-sterile soil demonstrated that ZA4 was significantly more abundant in seeds grown under non-sterile conditions (Fig. 3b), implying that ZA4 production is not regulated by developmental processes alone, but in response to biotic stimuli. Future efforts could test the hypothesis that scutella produce high levels of zealexins upon contact with the soil microbiome to protect the below ground organs of the germinating plant from detrimental microbes during the early stages of development.

The analysis of acidic sesquiterpenoids in different maize organs demonstrated variation in zealexin concentrations. The concentrations of ZA4 in the scutella reached levels  $> 8 \mu\text{g g}^{-1}$  FW across several diverse inbred lines tested, and were elicited to even higher levels in kernels infected with *A. flavus* ( $> 30 \mu\text{g g}^{-1}$  FW; Fig. 3; online resource S2). In comparing ZA4 with other zealexins, we observed that concentrations of ZA4 were generally lower than ZA1–ZA3 and ZB1 in the scutella and fungal-infected stem tissues (online resource S1; Huffaker et al. 2011), but became higher than the other zealexins at later time points in *A. flavus*-infected kernels (online resource S2), suggesting the enhanced processing of ZA1 and ZA3 during advanced disease progression. Collectively, these results demonstrate the variation in maize phytoalexin production from different treatments/organs and show that different zealexins may be regulated in a temporal-, organ-, and pathogen-specific manner.

The diverse levels of pathogen susceptibility to different zealexins demonstrate specificity for zealexin antimicrobial activity. For example, ZA4 had strong antimicrobial activity against *A. flavus* but only minimal action against *R. microsporus*. In previous analyses, other zealexins also displayed diverse inhibitory activity on fungal pathogens, as demonstrated by ZA1, ZA2, and ZA3 resulting in 80, 0, and 32% inhibition against *A. flavus*, respectively (Huffaker et al. 2011). Comparatively, ZA4 activity resulted in 31% inhibition of *A. flavus* growth. Similar differences were observed in liquid cultures of *R. microsporus*, where ZA4 showed no inhibition compared to strong growth inhibition (45%) exhibited by ZA1 (Huffaker et al. 2011). Collectively, these results demonstrate the diverse impacts of individual zealexins against fungal growth, and indicate that some pathogens may have an enhanced capacity to detoxify or tolerate specific zealexins. Furthermore, comparative analyses of all zealexins tested support the finding that ZA1 is the most potent antimicrobial zealexin against *A. flavus* and *R. microsporus*. Structural comparisons show that the major difference between ZA1 and ZA2–ZA4 is the addition of an oxygen moiety. Although variance in the position and oxidation state of the oxygen exists, the

general presence of additional oxygens on the ZA1 derivatives may explain the reduced antimicrobial potency of these compounds. A possible biological impetus behind the modification of ZA1 may be that divergent zealexins act synergistically to thwart biotic attack. Another alternative is that ZA2, ZA3, and ZA4 may be less-active derivatives of ZA1, a mechanism for the plant to reduce autotoxicity associated with high ZA1 concentrations. It is also possible that zealexin variants exist to hinder the ability of pathogens to detoxify single compounds and rapidly acquire resistance.

In addition to fungal-elicited responses, levels of ZA4 accumulate in the tissue surrounding *O. nubilalis* feeding sites. In support of the potential role for ZA4 and other zealexins in defense against herbivory are microarray results showing the significant induction of *Tps11* transcripts in response to *O. nubilalis* tunnel feeding (Dafoe et al. 2013). Additional evidence demonstrating the potential for non-volatile terpenoid defenses against maize herbivores was shown by the exogenous application of kauralexins to stem tissues, which resulted in antifeedant activity in paired choice assays (Schmelz et al. 2011). Collectively, these studies demonstrate that herbivore-inducible terpenoids could play a defensive role against stem boring insects.

As herbivore- and fungal-elicited maize acidic terpenoids have been shown to be affected by E-CO<sub>2</sub> (Vaughan et al. 2014, 2016), we investigated the impact of E-CO<sub>2</sub> on ZA4 production. Interestingly, both *O. nubilalis*- and *A. flavus*-induced levels of ZA4 were significantly attenuated in plants grown under E-CO<sub>2</sub> conditions. The effect of E-CO<sub>2</sub> on ZA4 production in maize kernels following *A. flavus* elicitation aligns with previous observations in *F. verticillioides*-infected stems, where total zealexins and kauralexins were significantly reduced under E-CO<sub>2</sub> (Vaughan et al. 2014). The reduction of ZA4 and other biochemical defenses in response to pathogen and insect attack under E-CO<sub>2</sub>, as described in this and previous studies (Vaughan et al. 2014, 2016), supports the hypothesis that altered CO<sub>2</sub> levels may have a strong impact on plant defenses. While E-CO<sub>2</sub> alone can have a dampening effect on maize defense and promote susceptibility, it is difficult to predict how diverse abiotic stress conditions will impact maize production. For example, drought stress has been shown to offset the impact of E-CO<sub>2</sub> on defense systems, rendering soybean plants as resistant to pathogen attack as their counterparts under ambient CO<sub>2</sub> and irrigated conditions (Casteel et al. 2012). Yet in maize, the same compounding stresses (i.e. heightened CO<sub>2</sub> and drought stress) cause plants to be more susceptible to the stalk rot pathogen *F. verticillioides* (Vaughan et al. 2016). Elucidation of maize defense responses in plants exposed to combinations of biotic and abiotic stress will be required to better predict the impact of simultaneous stressors.

## Conclusions

While examining defense metabolite profiles in pathogen-infected maize, we identified a novel  $\beta$ -macrocarpene derivative, termed ZA4. The accumulation of ZA4 occurs ubiquitously in maize scutella during seedling development, but is not induced by developmental regulation alone. ZA4 is elicited by *A. flavus* and *R. microsporus* and displays antimicrobial activity against *A. flavus* in vitro. Production of ZA4 was also observed in response to infestation with the stem tunneling herbivore *O. nubilalis*. Fungal- and herbivore-elicited ZA4 in maize plants grown under E-CO<sub>2</sub> is significantly reduced compared to plants grown under ambient conditions, demonstrating a negative impact for E-CO<sub>2</sub> on plant defense. Collectively, the results from this study elucidate the production and function of a novel antimicrobial phytoalexin. As other members of this defensive metabolic network predictably exist, continued efforts will contribute to our knowledge of specific maize defenses and ultimately pathway genes that could be pursued using molecular breeding practices to strengthen resistance traits.

**Author contribution statement** SAC, AH, JEM, WPW, and EAS designed research; SAC, AH, JS, MV, CH, AB, JEM, WPW, and EAS performed research; SAC, JS, AH, MV, HA, MR and EAS contributed new reagents/analytical tools; SAC, DW, and EAS analyzed data; SAC, AH, and EAS interpreted the data; and SAC and EAS wrote the paper.

**Acknowledgements** We thank Dawn Diaz-Ruiz, Amanda Balon, Steve Willms, and Bevin Ferguson for their technical support. Special thanks to James R. Rocca for facilitating NMR experiments at the University of Florida McKnight Brain Institute (National High Magnetic Field Laboratory AMRIS Facility) supported by NSF-DMR award 1157490, the State of Florida, and NIH award S10RR031637. Mention of trade names or commercial products in this publication is solely for the purpose of providing specific information and does not imply recommendation or endorsement by the USDA. Research was funded by US Department of Agriculture (USDA)-Agricultural Research Service Project 6036-21000-011-00D, and by NSF Division of Integrative Organismal Systems Competitive Award 1139329.

## Compliance with ethical standards


**Conflict of interest** The authors declare no conflict of interest.

## References

- Ahuja I, Kissen R, Bones AM (2012) Phytoalexins in defense against pathogens. *Trends Plant Sci* 17(2):73–90. <https://doi.org/10.1016/j.tplants.2011.11.002>
- Basse CW (2005) Dissecting defense-related and developmental transcriptional responses of maize during *Ustilago maydis* infection and subsequent tumor formation. *Plant Physiol* 138(3):1774–1784. <https://doi.org/10.1104/pp.105.061200>
- Casteel CL, Niziolek OK, Leakey ADB, Berenbaum MR, DeLucia EH (2012) Effects of elevated CO<sub>2</sub> and soil water content on phytohormone transcript induction in *Glycine max* after *Popillia japonica* feeding. *Arthropod Plant Int* 6(3):439–447. <https://doi.org/10.1007/s11829-012-9195-2>
- Chakraborty S, Newton AC (2011) Climate change, plant diseases and food security: an overview. *Plant Pathol* 60(1):2–14. <https://doi.org/10.1111/j.1365-3059.2010.02411.x>
- Chandlee JM, Scandalios JG (1984) Analysis of variants affecting the catalase developmental program in maize scutellum. *Theor Appl Genet* 69(1):71–77. <https://doi.org/10.1007/bf00262543>
- Christensen S, Borrego E, Shim WB, Isakeit T, Kolomiets M (2012) Quantification of fungal colonization, sporogenesis, and production of mycotoxins using kernel bioassays. *J Vis Exper*. <https://doi.org/10.3791/3727>
- Christensen SA, Huffaker A, Kaplan F, Sims J, Ziemann S, Doehlemann G, Ji L, Schmitz RJ, Kolomiets MV, Alborn HT, Mori N, Jander G, Ni X, Sartor RC, Byers S, Abdo Z, Schmelz EA (2015) Maize death acids, 9-lipoxygenase-derived cyclopentane(a) nones, display activity as cytotoxic phytoalexins and transcriptional mediators. *Proc Natl Acad Sci USA* 112(36):11407–11412. <https://doi.org/10.1073/pnas.1511131112>
- Corona-Carrillo JI, Flores-Ponce M, Chavez-Najera G, Diaz-Pontones DM (2014) Peroxidase activity in scutella of maize in association with anatomical changes during germination and grain storage. *Springerplus* 3:399. <https://doi.org/10.1186/2193-1801-3-399>
- Dafoe NJ, Thomas JD, Shirk PD, Legaspi ME, Vaughan MM, Huffaker A, Teal PE, Schmelz EA (2013) European corn borer (*Ostrinia nubilalis*) induced responses enhance susceptibility in maize. *PLoS One* 8(9):e73394. <https://doi.org/10.1371/journal.pone.0073394>
- Doehlemann G, Wahl R, Horst RJ, Voll LM, Usadel B, Poree F, Stitt M, Pons-Kuhnemann J, Sonnewald U, Kahmann R, Kamper J (2008) Reprogramming a maize plant: transcriptional and metabolic changes induced by the fungal biotroph *Ustilago maydis*. *Plant J* 56(2):181–195. <https://doi.org/10.1111/j.1365-313X.2008.03590.x>
- Gatch EW, Munkvold GP (2002) Fungal species composition in maize stalks in relation to European corn borer injury and transgenic insect protection. *Plant Dis* 86(10):1156–1162. <https://doi.org/10.1094/pdis.2002.86.10.1156>
- Greer S, Wen M, Bird D, Wu X, Samuels L, Kunst L, Jetter R (2007) The cytochrome P450 enzyme CYP96A15 is the midchain alkane hydroxylase responsible for formation of secondary alcohols and ketones in stem cuticular wax of Arabidopsis. *Plant Physiol* 145(3):653–667. <https://doi.org/10.1104/pp.107.107300>
- Harris LJ, Saparno A, Johnston A, Priscic S, Xu M, Allard S, Kathiresan A, Ouellet T, Peters RJ (2005) The maize *An2* gene is induced by *Fusarium* attack and encodes an ent-copalyl diphosphate synthase. *Plant Mol Biol* 59(6):881–894. <https://doi.org/10.1007/s11103-005-1674-8>
- Huffaker A, Kaplan F, Vaughan MM, Dafoe NJ, Ni X, Rocca JR, Alborn HT, Teal PEA, Schmelz EA (2011) Novel acidic sesquiterpenoids constitute a dominant class of pathogen-induced phytoalexins in maize. *Plant Physiol* 156(4):2082–2097. <https://doi.org/10.1104/pp.111.179457>
- Keller NP, Bergstrom GC, Carruthers RI (1986) Potential yield reductions in maize associated with an anthracnose european corn-borer pest complex in new-york. *Phytopathology* 76(6):586–589. <https://doi.org/10.1094/Phyto-76-586>
- Kobayashi T, Ishiguro K, Nakajima T, Kim HY, Okada M, Kobayashi K (2006) Effects of elevated atmospheric CO<sub>2</sub> concentration

- on the infection of rice blast and sheath blight. *Phytopathology* 96(4):425–431. <https://doi.org/10.1094/phyto-96-0425>
- Kollner TG, Schnee C, Li S, Svatos A, Schneider B, Gershenzon J, Degenhardt J (2008) Protonation of a neutral (*S*)-beta-bisabolene intermediate is involved in (*S*)-beta-macrocarpene formation by the maize sesquiterpene synthases TPS6 and TPS11. *J Biol Chem* 283(30):20779–20788. <https://doi.org/10.1074/jbc.M802682200>
- Mao H, Liu J, Ren F, Peters RJ, Wang Q (2016) Characterization of CYP71Z18 indicates a role in maize zealexin biosynthesis. *Phytochemistry* 121:4–10. <https://doi.org/10.1016/j.phytochem.2015.10.003>
- Melloy P, Hollaway G, Luck J, Norton R, Aitken E, Chakraborty S (2010) Production and fitness of *Fusarium pseudograminearum* inoculum at elevated carbon dioxide in FACE. *Glob Change Biol* 16(12):3363–3373. <https://doi.org/10.1111/j.1365-2486.2010.02178.x>
- Mueller DS, Wise KA, Sisson AJ et al (2016) Corn yield loss estimates due to diseases in the United States and Ontario, Canada from 2012 to 2015. *Plant Health Progress* 17:211–222
- Oerke EC, Dehne HW, Shonbeck F, Weber A (1994) Crop production and crop protection. Estimated losses in major food and cash crops, vol 1. Elsevier, Amsterdam. ISBN 9780444597946
- Savary S, Ficke A et al (2012) Crop losses due to diseases and their implications for global food production losses and food security. *Food Secur* 4:519–537. <https://doi.org/10.1007/s12571-012-0200-5>
- Schmelz EA, Engelberth J, Alborn HT, Tumlinson JH, Teal PEA (2009) Phytohormone-based activity mapping of insect herbivore-produced elicitors. *Proc Natl Acad Sci USA* 106(2):653–657. <https://doi.org/10.1073/pnas.0811861106>
- Schmelz EA, Kaplan F, Huffaker A, Dafoe NJ, Vaughan MM, Ni X, Rocca JR, Alborn HT, Teal PE (2011) Identity, regulation, and activity of inducible diterpenoid phytoalexins in maize. *Proc Natl Acad Sci USA* 108(13):5455–5460. <https://doi.org/10.1073/pnas.1014714108>
- Schmelz EA, Huffaker A, Sims JW, Christensen SA, Lu X, Okada K, Peters RJ (2014) Biosynthesis, elicitation and roles of monoterpene phytoalexins. *Plant J* 79(4):659–678. <https://doi.org/10.1111/tpj.12436>
- Solomon SD, Qin D, Manning M et al (2007) Climate change 2007: the physical science basis. Contribution of working group I to the fourth assessment report of the intergovernmental panel on climate change. Cambridge University Press, Cambridge
- Strengbom J, Reich PB (2006) Elevated [CO<sub>2</sub>] and increased N supply reduce leaf disease and related photosynthetic impacts on *Solidago rigida*. *Oecologia* 149(3):519–525. <https://doi.org/10.1007/s00442-006-0458-4>
- van der Linde K, Kastner C, Kumlehn J, Kahmann R, Doehlemann G (2011) Systemic virus-induced gene silencing allows functional characterization of maize genes during biotrophic interaction with *Ustilago maydis*. *New Phytol* 189(2):471–483. <https://doi.org/10.1111/j.1469-8137.2010.03474.x>
- Vaughan MM, Huffaker A, Schmelz EA, Dafoe NJ, Christensen S, Sims J, Martins VF, Swerbilow J, Romero M, Alborn HT, Allen LH, Teal PE (2014) Effects of elevated [CO<sub>2</sub>] on maize defence against mycotoxigenic *Fusarium verticillioides*. *Plant Cell Environ* 37(12):2691–2706. <https://doi.org/10.1111/pce.12337>
- Vaughan MM, Huffaker A, Schmelz EA, Dafoe NJ, Christensen SA, McAuslane HJ, Alborn HT, Allen LH, Teal PEA (2016) Interactive effects of elevated [CO<sub>2</sub>] and drought on the maize phytochemical defense response against mycotoxigenic *Fusarium verticillioides*. *PLoS One* 11(7):e0159270. <https://doi.org/10.1371/journal.pone.0159270>
- Wang SM, Huang AHC (1987) Biosynthesis of lipase in the scutellum of maize kernel. *J Biol Chem* 262(5):2270–2274
- Wang W, Vinocur B, Altman A (2003) Plant responses to drought, salinity and extreme temperatures: towards genetic engineering for stress tolerance. *Planta* 218(1):1–14. <https://doi.org/10.1007/s00425-003-1105-5>
- Watanabe M, Kono Y, Esumi Y, Teraoka T, Hosokawa D, Suzuki Y, Sakurai A, Watanabe M (1996) Studies on a quantitative analysis of oryzalides and oryzalic acids in rice plants by GC–SIM. *Biosci Biotechnol Biochem* 60:1460–1463
- Yu JM, Holland JB, McMullen MD, Buckler ES (2008) Genetic design and statistical power of nested association mapping in maize. *Genetics* 178(1):539–551. <https://doi.org/10.1534/genetics.107.074245>

## Affiliations

Shawn A. Christensen<sup>1</sup>  · Alisa Huffaker<sup>2</sup> · James Sims<sup>3</sup> · Charles T. Hunter<sup>1</sup> · Anna Block<sup>1</sup> · Martha M. Vaughan<sup>4</sup> · Denis Willett<sup>1</sup> · Maritza Romero<sup>1</sup> · J. Erik Mylroie<sup>5</sup> · W. Paul Williams<sup>6</sup> · Eric A. Schmelz<sup>2</sup>

<sup>1</sup> Chemistry Research Unit, Center for Medical, Agricultural, and Veterinary Entomology, United States Department of Agriculture, Agricultural Research Service, Gainesville, FL 32608, USA

<sup>2</sup> Section of Cell and Developmental Biology, University of California at San Diego, La Jolla, CA 92093-0380, USA

<sup>3</sup> Department of Environmental Systems Science, ETH Zurich, 8092 Zurich, Switzerland

<sup>4</sup> Mycotoxin Prevention and Applied Microbiology Research, United States Department of Agriculture, Agricultural

Research Service, 1815 N. University St., Peoria, IL 61604, USA

<sup>5</sup> Bennett Aerospace, Engineer and Research Development Center, Vicksburg, MS 39180, USA

<sup>6</sup> Crop Science Research Laboratory, United States Department of Agriculture, Agricultural Research Service, Dorman Hall, Stone Blvd., Starkville, MS 39762, USA